

Zinc complexes of novel Schiff bases derived from 1,8-Diaminonaphthalene: Synthesis, characterization and biological activity evaluation

Walaa H. Mahmoud^a, Ahmed M. Refaat^a, Gehad G. Mohamed^{ab*}

^a Chemistry Department, Faculty of Science, Cairo University, Giza, 12613, Egypt

^b Egypt Nanotechnology Center, Cairo University, 6th October City, Giza, Egypt

Corresponding Author : Walaa H. Mahmoud

ABSTRACT: 1,8-Diaminonaphthalene on reaction with methyl 2-pyridyl ketone and 2-hydroxy-1-naphthaldehyde yielded new Schiff's base ligands (L^1 and H_2L^2). The coordination behavior of Zinc ion to form $[ZnL^1]$ and $[ZnH_2L^2]$ complexes have been established on the basis of analytical and spectral data including FT-IR, ¹HNMR, Mass, thermal and elemental analyses. The two complexes have octahedral geometries. The Schiff bases and Zn(II) metal complexes displays antibacterial properties.

KEY WORDS: 1,8-Diaminonaphthalene; Schiff base; spectral data; antibacterial.

Date of Submission: 16-01-2019

Date of acceptance: 28-01-2019

I. INTRODUCTION

Transition metal complexes with Schiff base ligands have played essential role in efficient catalysts [1], microbial and cancer drugs [2,3], sensors [4], nonlinear optic [5] and DNA cleavage performance fields [6]. Hence synthesis and characterization of Schiff base complexes have been widely investigated in coordination chemistry. Among these complexes, zinc Schiff base complexes have been receiving considerable attention for their fascinating applications [7-9]. Schiff bases containing heterocyclic structural units with N, N donor atoms are considered the most prominent research area in the field of coordination chemistry [10-12]. The various donor atoms in them offer special ability for binding metals. The incorporated metals in the lattice of donor atoms of Schiff base change the physiological, morphological, and pharmacological activities of the compounds. The heterocyclic based Schiff base is of promising research interest owing to the widespread antibacterial resistance of the medical science. Moreover, the revival of research is essential to generate new Schiff base metal complexes with a diverse range of applications. Schiff base complexes have been used as drugs and have valuable antibacterial [13,14], antifungal [15-17], antiviral [18,19], anti-inflammatory [20], and antitumor activities [21]. Zinc Schiff base complexes are a new class of luminescent compounds which showed photoluminescence properties [22]. Also, because of their catalytic properties, they are used as models of biological significance [23-25]. As in recent years, synthesis of materials in nano-scale has been increasing based on the fact that the reduction in particle size to nanometer scale results in high surface to volume ratio, change in electronic structure of materials that shows fascinating physical and chemical properties that are different from the bulk materials such as the mechanical, optical, and magnetic properties [26,27]. Schiff bases derived from substituted salicylaldehydes and amides showed a variety of biological activities [28, 29]. Schiff bases play important roles in coordination chemistry related to catalysis and enzymatic reactions, magnetism and molecular architecture [30,31], and also exhibit biological activities such as antimicrobial [32, 33]. The antibacterial activities against *Bacillus subtilis* (Gram-positive), *Staphylococcus aureus* (Gram-positive), *Escherichia coli* (Gram-negative), *Pseudomonas fluorescens* (Gram-negative) were studied. On the basis of the above considerations, we here report the synthesis, characterization and antibacterial activity of two new zinc(II) complexes based on Schiff base ligands.

II. EXPERIMENTAL

2.1 Materials and reagents:

All the chemicals used were of the analytical reagent grade (AR), and of highest purity available. They included 1,8-Diaminonaphthalene, methyl 2-pyridyl ketone, 2-hydroxy-1-naphthaldehyde, $ZnCl_2$ which were provided from (Merck, Germany), (Sigma Aldrich) and BDH respectively. Organic solvents used were ethyl alcohol (95 %), methyl alcohol and N,N-dimethylformamide (DMF). Deionized water was usually used in all preparations.

2.2 | Solutions

Stock solutions of the Schiff base ligands and its metal complexes of $1 \times 10^{-3} M$ were prepared by dissolving an accurately weighed amount in N,N-dimethylformamide. The conductivity then measured for the metal complexes solutions. Dilute solutions of the Schiff base ligands and its metal complexes ($1 \times 10^{-4} M$) were prepared by accurate dilution from the previous prepared stock solutions for measuring their UV-Vis spectra.

2.3 | Instrumentation

Microanalyses of carbon, hydrogen and nitrogen were carried out at the Microanalytical Center, Cairo University, Egypt, using a CHNS-932 (LECO) Vario elemental analyser. Analyses of the metals were conducted by dissolving the solid complexes in concentrated HNO_3 , and dissolving the residue in deionized water. The metal content was carried out using inductively coupled plasma atomic absorption spectrometry (ICP-AES), Egyptian Petroleum Research Institute. Fourier transform infrared (FT-IR) spectra were recorded with a PerkinElmer 1650 spectrometer ($400-4000\text{ cm}^{-1}$) in KBr pellets. 1H -NMR spectra, as solutions in $DMSO-d_6$, were recorded with a 300 MHz Varian-Oxford Mercury at room temperature using tetra-methylsilane as an internal standard. Mass spectra were recorded using the electron ionization technique at 70 eV with an MS-5988 GS-MS Hewlett-Packard instrument at the Microanalytical Center, National Center for Research, Egypt. UV-visible spectra were obtained with a Shimadzu UVmini-1240 spectrophotometer. Molar conductivities of $10^{-3} M$ solutions of the solid complexes in DMF were measured using a Jenway 4010 conductivity meter. Thermogravimetric (TG) and differential thermogravimetric (DTG) analyses of the solid complexes were carried out from room temperature to $1000\text{ }^\circ C$ using a Shimadzu TG-50H thermal analyzer. Antimicrobial measurements were carried out at the Microanalytical Center, Cairo University, Egypt.

2.4 Synthesis of Schiff base (L_1 and H_2L_2) ligands

Two Schiff base ligands were synthesized by refluxing of Methyl-2-pyridyl ketone (0.025 mol, 3g) with 1,8-Diaminonaphthalene (0.025 mol, 4 g) to give L_1 and 2-hydroxy-1-naphthaldehyde (0.025 mol, 4.3 g) with the same no. of moles of 1,8-Diaminonaphthalene dissolved in ethanol to form H_2L_2 . The resulting mixture was stirred under reflux for about 2 hours during which a brown L_1 and violet H_2L_2 solid compounds were separated. They were filtered, recrystallized and washed with diethyl ether and dried in vacuum.

2.5 Synthesis of the metal chelates

The metal complexes were prepared by the addition of hot solution ($60\text{ }^\circ C$) of the zinc chloride (0.83 mmol) and (0.77 mmol) in an ethanol (25 mL) to the hot solution ($60\text{ }^\circ C$) of the L^1 (0.4 g/L, 0.83 mmol) and H_2L^2 (0.4 g/L, 0.77 mmol) ligands in ethanol (25 mL), respectively. The formed mixture was stirred under reflux for two hours where upon the complexes precipitated. They were obtained by filtration, washed with a little amount of hot DMF and dried in vacuum desiccator over anhydrous calcium chloride. The analytical data for C, H and N were repeated twice.

III. PHARMACOLOGY

3.1 Antimicrobial activity

A filter paper disk (5 mm) was transferred into 250 ml flasks containing 20 mL of working volume of tested solution (100 mg/mL). All flasks were autoclaved for 20 min at $121\text{ }^\circ C$. LB agar media surfaces were inoculated with four investigated bacteria (Gram positive bacteria: Bacillus Subtilis and Streptococcus pneumoniae; Gram negative bacteria: Salmonella SP. And Escherichia coli) and fungi (Aspergillus fumigates and Candida albicans) by diffusion agar technique [34-36] then, transferred to a saturated disk with a tested solution in the center of Petri dish (agar plates). All the compounds were placed at 4 equidistant places at a distance of 2 cm from the center in the inoculated Petri plates. DMSO served as control. Finally, all these Petri dishes were incubated at $25\text{ }^\circ C$ for 48 h where clear or inhibition zones were detected around each disk. Control flask of the experiment was designed to perform under the same condition described previously for each microorganism but with dimethylformamide solution only and by subtracting the diameter of inhibition zone resulting with dimethylformamide from that obtained in each case, so antibacterial activity could be calculated

[34,35]. Amikacin and ketokonazole were used as reference compounds for antibacterial and antifungal activities, respectively. All experiments were performed as triplicate and data plotted were the mean value.

IV. RESULTS AND DISCUSSION

4.1 Characterization of the Schiff base ligands

The brown Schiff base ligand (L^1) and the violet Schiff base ligand (H_2L^2) were prepared by the self-condensation reaction of Methyl-2-pyridyl ketone (For L^1) and 2-hydroxy-1-naphthaldehyde (For H_2L^2) with 1,8-Diaminonaphthalene using ethanol as a solvent, the formed Schiff base ligands were steady in air and soluble in various organic solvents. The data obtained from the elemental analysis of C, H and N content of L^1 and H_2L^2 referred to ($C_{17}H_{15}N_3$) and ($C_{32}H_{22}N_2O_2$) were shown as C, 78.46 and 82.22; H, 5.72 and 4.52; N, 16.09 and 6.09, calculated: C, 78.16 and 82.40; H, 5.78 and 4.72; N, 15.91 and 6.00, respectively, there was good agreement between both of the experimental and theoretical data which prove the proposed formula.

Preparation of L^1 and H_2L^2 ligands were confirmed by the appearance of a strong IR band at 1595 and 1600 cm^{-1} , respectively, resulting from the formation of azomethine ($\nu(C=N)$) group [39]. The $\nu(OH)$ stretching band of H_2L^2 was observed at 3378 cm^{-1} , on the other hand, the $\nu(NH_2)$ bending band of L^1 was appeared at 625 cm^{-1} .

The proton 1H NMR spectrum was recorded for L^1 ligand the aromatic protons have been appeared as a set of multiplet in the region 6.64 – 7.89 ppm and the NH_2 proton appeared as singlet at the region 6.22 ppm. While in the case of the H_2L^2 ligand, the aromatic OH proton appeared as singlet signal at 10.9 ppm, the aromatic protons showed multiplet signal at the region of 6.80 – 7.95 ppm and the CH proton appeared as singlet signal at 9.09 ppm. The structures of the proposed Schiff base ligands were illustrated in Figure (1).

Figure 1. The proposed structure of (a) L^1 and b) $Zn(II)-L^1$ complex.

4.2 Characterization of metal complexes

All of the formed complexes were stable to air. They were soluble in many organic solvents including ethanol. The complexes were characterized by different techniques such as elemental analyses, 1H NMR, IR spectral and thermal analysis. The structure of the formed complexes was demonstrated in Figure (2).

Figure 2. The proposed structure of (a) H_2L^2 and b) $Zn(II)-H_2L^2$ complex.

4.3 Elemental analysis

Both experimental and theoretical results of the elemental analysis of the synthesized complexes have a high degree of accordance to each other which point out that the metal complexes of Schiff base ligands were formed in 1:1 ratio. The results of elemental analyses of $Zn(II)$ metal complexes (C, H, N, Cl and M) and melting point were scheduled in Table (1)

4.4 Infrared spectra and mode of bonding

The infrared spectral data for the Schiff base ligands and their metal complexes. The free L^1 and H_2L^2 ligands FT-IR spectra were matched with that of the formed complexes in order to allocate the coordination sites resulting in the chelation process.

The FT-IR spectra of the metal complex of H_2L^2 ligand showed a broad band around 3389cm^{-1} which may be assigned to $\nu(\text{OH})$, while it appears in H_2L^2 ligands spectra at 3378cm^{-1} , respectively. The ligands FT-IR spectra spectacle a distinguishable absorption band at 1595 and 1600cm^{-1} , that may be attributed to $\nu(\text{C}=\text{N})$ of azomethine group; on the other hand, this band was shifted to a higher or lower wavelength in the metal complexes and it appeared at the range $1611-1620\text{cm}^{-1}$. It was perceived that the $\nu(\text{NH}_2)$ bending band was appeared at 625cm^{-1} for L^1 ligand, while in the $Zn(II)$ metal complex, it was shifted to appear in the range of 631cm^{-1} as per that the stretching band of $\nu(\text{NH}_2)$ wasn't be able to described because of its

Table (1). Analytical and physical data of L^1 and H_2L^2 ligands and their $Zn(II)$ complexes.

Compound (Molecular Formula)	Colour	M.p. ($^{\circ}\text{C}$)	% Found (Calcd.)				Yield %	MW (gm/mol)	μ_{eff} (B.M.)	Δm $\Omega\text{-1mol-1}$ cm^2
			C	H	N	M				
Ligand (L^1)	Brown	188	78.42 (78.16)	5.78 (5.74)	15.91 (16.09)	-----	89	261	-----	-----
$[Zn(L^1)(H_2O)Cl_2] \cdot 2H_2O$	Brown	280	48.32 (48.11)	4.65 (5.42)	9.67 (9.90)	15.12 (15.33)	84	406	Diam.	44
Ligand (H_2L^2)	Violet	75	82.22 (82.40)	4.52 (4.72)	6.09 (6.00)	-----	88	466	-----	-----
$[Zn(H_2L^2)Cl_2] \cdot 2H_2O$	Reddish brown	166	60.22 (60.18)	4.20 (4.07)	4.29 (4.38)	10.24 (10.18)	87	638	Diam.	36

intersecting with $\nu(\text{OH})$ stretching band. The coordinating water molecules in the complexes are characterized by the occurrence of two bands at 853–939 and 750–850 cm^{-1} [40]. The synchronization of the nitrogen of the azomethine (imine) group is established by the presence of a new metal–ligand weak band at 421–485 cm^{-1} due to $\nu(\text{M-N})$ [41]. Another new weak band at 541 cm^{-1} has appeared which might be attributed to the formation of M-O bond in the metal complex of H_2L^2 ligand complex [42]. It was concluded from the previous data that the prepared L^1 ligand acts as a neutral tridentate ligand that binds to the metal ion through two nitrogen atoms (azomethine nitrogen and amino nitrogen) while H_2L^2 ligand acts as a neutral tetradentate ligand that binds to the metal ion through two azomethine nitrogen atoms and two phenolic oxygen atoms.

4.5 ^1H NMR spectral studies of the metal complexes

Upon matching the proton signals position in the Zn(II) complexes with those of the free ligands, it can be detected that all signals were in the expected region but only showed a slight shift due to the coordination of the ligand to the metal ion [14]. The multiplet signals in the region 6.64–7.89 and 6.8–7.95 ppm in L^1 and H_2L^2 ligands, respectively, may be attributed to aromatic protons [43,44], on the other hand, they appeared at 6.88–7.91 and 6.91–8.08 ppm in $[\text{Zn}(\text{L}^1)(\text{H}_2\text{O})\text{Cl}_2] \cdot 2\text{H}_2\text{O}$ and $[\text{Zn}(\text{H}_2\text{L}^2)\text{Cl}_2] \cdot 2\text{H}_2\text{O}$ complexes, respectively. The singlet signal observed at 6.22 ppm in the ^1H NMR spectrum of L^1 ligand, which may be corresponded to the NH_2 proton, has appeared in the spectrum of formed Zn(II) complex $[\text{Zn}(\text{L}^1)(\text{H}_2\text{O})\text{Cl}_2] \cdot 2\text{H}_2\text{O}$ at 6.29 ppm. The singlet signal in the region 10.95 ppm in the Schiff base ligand H_2L^2 which may be attributed to Aromatic OH group, was shifted to 10.98 ppm in $[\text{Zn}(\text{H}_2\text{L}^2)\text{Cl}_2] \cdot 2\text{H}_2\text{O}$ complex that proved that coordination of zinc ion to phenolic oxygen without deprotonating.

4.6 Molar conductance measurements

The solubility of the complexes in ethanol allowed the determination of the molar conductivity (Λ_m) of 10^{-3} M solutions for all complexes at 25°C. It was concluded from the results that $[\text{Zn}(\text{L}^1)(\text{H}_2\text{O})\text{Cl}_2] \cdot 2\text{H}_2\text{O}$ and $[\text{Zn}(\text{H}_2\text{L}^2)\text{Cl}_2] \cdot 2\text{H}_2\text{O}$ complexes had molar conductance values of 44 and 36 $\Omega^{-1} \text{mol}^{-1} \text{cm}^2$, respectively, indicating their weak ionic nature (non-electrolytes). This confirmed that the anions were involved in the coordination sphere [45]. The molar conductance data was demonstrated in Table (1).

4.7 Thermal analysis studies (TGA and DTG)

The thermogravimetric technique (TG) and differential thermogravimetric (DTG) analyses for the L^1 and H_2L^2 ligands and its metal complexes were explained in Table (2) within the temperature range from 45 to 1000 °C. The TG data for L^1 Schiff base ligand showed three decomposition platforms. The first stage within the temperature range of 45–310 °C and a maximum temperature of 256 °C, which resembles to the evaluation of $\text{C}_3\text{H}_8\text{N}$ molecule with mass loss of 22.28 % (calculated mass loss = 22.23%). The second decomposition step was found within the temperature range of 310–1000 °C and a maximum temperature of 760 °C, which corresponds to the loss of $\text{C}_{14}\text{H}_7\text{N}_2$ molecule with mass loss of 76.15 % (calculated mass loss = 76.59 %). The DTG curve provided maximum peak temperature at 760 °C and the total weight loss amounted to 98.43 % (calcd. 98.82 %). The thermogravimetric (TG) curve for $[\text{Zn}(\text{L}^1)(\text{H}_2\text{O})\text{Cl}_2] \cdot 2\text{H}_2\text{O}$ complex displayed four weight loss steps in the temperature range of 44–1000 °C. The first stage of decomposition arisen within the range of 45–224 °C, with a temperature maximum at 103 °C which related to the loss of the water molecule of hydration and CH_4 , with estimated mass loss of 13.09 % (calculated mass loss = 12.26%). The next step of decomposition was detected within the range of 224–375 °C, with a temperature maximum at 270 °C that may be attributed to the loss of the one molecule of coordinated water, Cl_2 molecule and HCN molecule, where the mass loss was found to be 25.34 % (calculated mass loss = 26.88 %). The third stage of decomposition was observed within the range of 375–998 °C, with a temperature maximum at 502 °C and corresponds to the loss of a $\text{C}_9\text{H}_{13}\text{N}_2$ molecule with an estimated mass loss of 36.44 % (calculated mass loss = 35.14%). The overall weight loss was evaluated as 74.89 % (calculated mass loss = 74.28 %) leaving ZnO metal oxide with remaining carbon as a residue. The TG data for H_2L^2 Schiff base ligand showed three stages of decomposition. The first stage within the temperature range of 45–167 °C with a temperature maximum of 76 °C, which corresponded to the evaluation of C_2H_6 molecule with mass loss of 6.47 % (calculated mass loss = 6.43 %). The second and third decomposition steps were found within the temperature range of 167–1000 °C and a temperature maximum of 690 °C, which corresponds to the loss of $\text{C}_{30}\text{H}_{16}\text{N}_2\text{O}_2$ molecule with mass loss of 93.34 % (calculated mass loss = 92.81%). The DTG curve gave maximum peak temperature at 690 °C and the total weight loss amounted to 98.81 % (calcd. 99.98 %).

Table (2). Thermoanalytical results (TG and DTG) of oL^1 and H_2L^2 and Zn(II) complexes.

Complex	TG range (°C)	DTG _{max} (°C)	n*	Mass loss Estim (Calcd) %	Total mass loss %	Assignment	Residues
L^1	45-310	256	1	22.28 (22.23)		- Loss of $\text{C}_2\text{H}_5\text{N}$.	
	310-1000	740	1	76.15 (76.59)	98.43 (98.82)	-Loss of $\text{C}_{14}\text{H}_7\text{N}_2$
$[\text{Zn}(\text{L}^1)(\text{H}_2\text{O})\text{Cl}_2] \cdot 2\text{H}_2\text{O}$	44-224	103	1	13.09 (12.26)		-Loss of CH_4 and $2\text{H}_2\text{O}$.	
	224-373	270	1	25.34 (26.88)		-Loss of Cl_2 , HCN and H_2O .	$\text{ZnO}+6\text{C}$
	373-998	502	1	36.44 (35.14)	74.89 (74.28)	-Loss of $\text{C}_9\text{H}_{12}\text{N}_2$.	
H_2L^2	45-167	76	1	6.47 (6.43)		-Loss of C_2H_6 .	
	167-1000	184, 690	2	93.34 (92.81)	98.81 (100.00)	-Loss of $\text{C}_{10}\text{H}_{16}\text{N}_2\text{O}_2$
$[\text{Zn}(\text{H}_2\text{L}^2)\text{Cl}_2] \cdot 2\text{H}_2\text{O}$	45-224	93	1	10.83 (11.28)		-Loss of $\frac{1}{2}\text{Cl}_2$ and $2\text{H}_2\text{O}$.	
	224-501	291, 452	2	21.44 (21.94)		-Loss of $\frac{1}{2}\text{Cl}_2$ and $\text{C}_6\text{H}_4\text{N}_2$.	$\text{ZnO}+11\text{C}$
	501-998	744	1	38.47 (37.49)	74.76(74.52)	-Loss of $\text{C}_{17}\text{H}_{18}\text{O}$.	

The thermogravimetric (TG) curve for $[\text{Zn}(\text{H}_2\text{L}^2)\text{Cl}_2] \cdot 2\text{H}_2\text{O}$ complex exhibited four weight loss steps in the temperature range of 50-998 °C. The first step of decomposition occurred within the range of 50-224 °C, with a temperature maximum at 93 °C which corresponds to the loss of the two water molecules of hydration and half Chlorine molecule with estimated mass loss of 10.83% (calculated mass loss = 11.28%). The next two step of decomposition were observed within the range of 224-501 °C, with a temperature maximum at 291 and 452 °C that may be related to the loss of the half Chlorine molecule along with $\text{C}_6\text{H}_4\text{N}_2$ fragment, where the mass loss was found to be 21.44% (calculated mass loss = 21.94%). The final stage of decomposition was observed within the range of 501-998 °C, with a temperature maximum at 744 °C and corresponds to the loss of a $\text{C}_{17}\text{H}_{18}\text{O}$ molecule with an estimated mass loss of 38.47% (calculated mass loss = 37.49%) leaving ZnO metal oxide with remaining carbon as a residue. The overall weight loss was evaluated as 74.76% (calculated mass loss = 74.52%).

4.8 Structural interpretation

The structures of the synthesized metal complexes of L^1 and H_2L^2 ligands with Zn(II) metal were characterized by elemental analyses, molar conductance, magnetic and thermal analysis techniques. From the elemental analysis, it was established that the two ligands and their complexes were soluble in ethanol and the complexes formed by 1:1 ratio. From IR and ^1H NMR spectra, it could be concluded that L^1 ligand behaved as a neutral tridentate ligand while H_2L^2 ligand acted as neutral tetradentate ligand. From the molar conductance data, it was found that both the two Zn(II) complexes are non-electrolytes. Finally, the octahedral structure of the complexes was proved (Figures 1 and 2).

4.9 Biological activity

The prepared Zn(II) metal complexes have higher antibacterial activity than that of the free ligands which can be related to the chelation of the Schiff base with metal ions [46] as metal chelates displaying both polar and nonpolar properties; this creates a proper molecules for the penetration into cells and tissues. The polarity of the metal ion will be reduced to a greater extent because of the overlap of the ligand orbital upon chelation process, and partial sharing of the positive charge of the metal ion with donor groups [47,48]. Chelation enriches the delocalization of π -electrons over the whole chelating ring and prompts the penetration of the complexes into lipid membranes [46]. It also increases the lipophilic and hydrophilic nature of the central metal ions contributing in liposolubility and permeability through the lipid layer of cell membranes. As well as, lipophilicity, which accountable for the molecules entry rate into the cell, is enhanced by coordination, so the metal complex can become more active than the free Schiff base ligands.

Schiff base ligands and their complexes were screened for antibacterial and fungicidal activities. The results was recorded in Table (3) and Figure (3) showed that complexes displayed more inhibitory effects than the parent ligand. Antibacterial activity was tested in vitro against *Streptococcus aureus*; *Bacillus Subtilis*; *Salmonella SP.* and *Escherichia coli*.

The antibacterial studies showed that, by using *Streptococcus aureus* Gram-positive bacteria, the both the two ligands and it's the metal complexes recorded their biological activity. Using *Bacillus Subtilis* Gram-positive

bacteria, the H_2L^2 ligand and both metal complexes biological activity towards it, while L^1 ligand haven't any biological activity toward it. On the other hand, $[Zn(L^1)(H_2O)Cl_2].2H_2O$, and $[Zn(H_2L^2)Cl_2].2H_2O$ complexes showed a biological activity but $[Zn(H_2L^2)Cl_2].2H_2O$ complex was the highest of them.

Using Salmonella SP. as Gram-negative bacteria, $[Zn(H_2L^2)Cl_2].2H_2O$ complex has the highest biological activity of all of them. Using Escherichia coli as Gram-negative

bacteria, all of them recorded their biological activity towards it as mentioned in Table (3).

For fungicidal activity, compounds were screened in vitro against Aspergillus fumigatus and Candida albicans. The antifungal studies showed, by using Candida albicans, $[Zn(H_2L^2)Cl_2].2H_2O$ complex showed the highest biological activity while $[Zn(H_2L^2)(H_2O)_2Cl_2].2H_2O$ complex record low activity. Using Aspergillus fumigatus, the highest biological activity was that of the $[Zn(H_2L^2)Cl_2].2H_2O$ complex and the lowest activity was that of the $[Zn(H_2L^2)(H_2O)Cl_2].2H_2O$ complex. while there wasn't any biological activity for the H_2L^2 ligand [49].

From the previous data, it is concluded that Zn(II) complexes had the highest activity index in most cases.

V. SUMMARY AND CONCLUSION

Novel Schiff base L^1 and H_2L^2 ligands were synthesized as the condensation product subsequent from the reaction between methyl 2-pyridyl ketone and 2-hydroxy-1-naphthaldehyde with 1,8-diaminonaphthalene, respectively. Zn(II) metal were coordinated with the Schiff base ligands, where all the resulting complexes evidenced to be of the MHL type and were formed by 1:1 ratio of metal salt: ligand, as

Table (3). Biological activity of Schiff base ligands (L^1 and H_2L^2) and Zn(II) complexes.

	Inhibition zone diameter (mm / mg sample)					
	(Gram positive)		(Gram negative)		(fungus)	
	Bacillus Subtilis	Streptococcus pneumoniae	Escherichia Coli	Salmonella SP	Aspergillus fumigates	Candida albicans
L^1	0	15	0	12	9	11
$[Zn(L^1)(H_2O)Cl_2].2H_2O$	16	18	17	12	14	11
H_2L^2	9	15	11	16	0	0
$[Zn(H_2L^2)Cl_2].2H_2O$	15	20	18	16	19	23
Amphotericin	-----	-----	-----	-----	24	25
Ampicillin	32	25	-----	-----	-----	-----
Getamicin	-----	-----	20	17	-----	-----

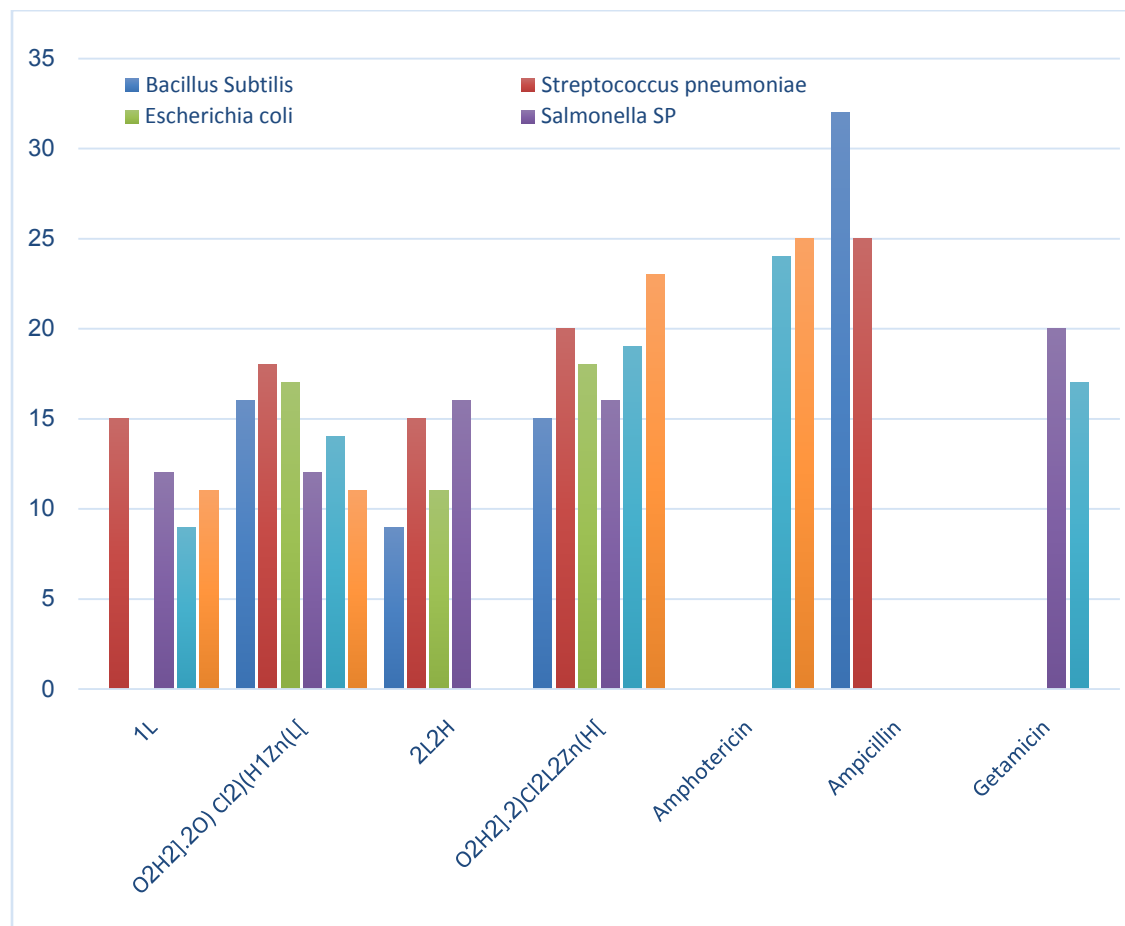


Figure 3. Biological activity of Schiff base ligands (L^1 and H_2L^2) and their Zn(II) complexes.

confirmed by the elemental analysis. Both of the IR and 1H NMR spectra have indeed confirmed that the L^1 ligand behaves as a neutral tridentate ligand that coordinates to the metal ions via three nitrogen atoms (the two azomethine nitrogens as well as the amino nitrogen) while H_2L^2 ligand acts as a neutral tetradentate ligand that binds to the metal ion through two nitrogen atoms (azomethine nitrogen) and two phenolic oxygens. The expected general formula of the formed complexes is $[M(L)(H_2O)_xCl_y]Cl_n \cdot (H_2O)_m$. Zn(II) complexes are determined as non-electrolytes, as shown by conductimetric measurements. On the other hand, the molar conductance. All the complexes exhibited octahedral geometry. The antimicrobial activity test proved that Zn(II) complex of H_2L^2 Ligand had the highest activity index. Therefore, the results of this present study will hopefully facilitate the research for the synthesis and application of novel metal complexes based on the newly prepared Schiff bases.

Competing Interest

None of the authors have any competing interests in the manuscript

REFERENCES

- [1]. Karunakaran C., Dhanalakshmi R., (2009), Selectivity in photo catalysis by particulate Semiconductors. Cent. Europ. J. Chem. 7: 134-138.
- [2]. Rayati S., Zakavi S., Koliaei M., Wojtczak A., Kozakiewicz A., (2010), A comparison with electron deficient ones. Inorg. Chem. Commun. 13: 203-207.
- [3]. Jeslin Kanagalamba P., Annaraj B., Thalamuthu S., Neelakantan M. A., (2013), Spectrochim. Acta: Part A. 104: 300-309.
- [4]. Patterson A. E., Miller J. J., Miles B. A., Stewart E. L., Melanson J. M. E. J., Vogels C. M., Cockshutt A. M., Decken A., Jr P. M., Westcott S. A., (2014), Inorg. Chim. Acta. 415: 88-94.
- [5]. Emadi D., Ya-ian M. R., Rayati S., (2007), Turk. J. Chem. 31: 423-433.
- [6]. Ebrahimipour S. Y., Sheikhshoaei I., Crochet A., Khaleghi M., Fromm K. M., (2014), J. Molec. Struct. 1072: 267-276.
- [7]. Routier S., Vezin H., Lamour E., Bernier J. L., Catteau J. P., Bailly C., (1999), Res. 27: 4160-4166.
- [8]. Mohamed G. G., Moma, M. M., Hindy A. M., (2006), Turk. J. Chem. 30: 361-382.
- [9]. Karekal M. R., Bennikallu Hire Mathad M., (2013), Turk. J. Chem. 37: 775-795.

- [10]. M. Gulcan, S. Ozdemir, A. D'undar, E. Ispir, and M. Kurtoğlu, *Zeitschrift für Anorganische und Allgemeine Chemie*, vol. 640, no. 8-9, pp. 1754–1762, 2014.
- [11]. M. S. Nair, D. Arish, and R. S. Joseyphus, *Journal of Saudi Chemical Society*, vol. 16, no. 1, pp. 83–88, 2012.
- [12]. W. Al Zoubi, A. A. S. Al-Hamdani, and M. Kaseem, *Applied Organometallic Chemistry*, vol. 30, no. 10, pp. 810–817, 2016.
- [13]. J. R. Anaconda, N. Noriega, and J. Camus, *Spectrochimica Acta - Part A: Molecular and Biomolecular Spectroscopy*, vol. 137, pp. 16–22, 2015.
- [14]. R. Nair, A. Shah, S. Baluja, and S. Chanda, *Journal of the Serbian Chemical Society*, vol. 71, no. 7, pp. 733–744, 2006.
- [15]. G. B. Bagihalli, P. G. Avaji, S. A. Patil, and P. S. Badami, *European Journal of Medicinal Chemistry*, vol. 43, no. 12, pp. 2639–2649, 2008.
- [16]. N. Raman, A. Sakthivel, and K. Rajasekaran, *Mycobiology*, vol. 35, no. 3, pp. 150–153, 2007.
- [17]. B. S. Creaven, E. Czegeledi, M. Devereux et al., *Dalton Transactions*, vol. 39, pp. 10854–10865, 2010.
- [18]. A. Jarrahpour, D. Khalili, E. De Clercq, C. Salmi, and J.
- [19]. M. Brunel, *Molecules*, vol. 12, pp. 1720–1730, 2007.
- [20]. S. K. Bharti, S. K. Patel, G. Nath, R. Tilak, and S. K. Singh, *Transition Metal Chemistry*, 2010.
- [21]. M. Manjunatha, V. H. Naik, A. D. Kulkarni, and S. A. Patil, *Journal of Coordination Chemistry*, vol. 64, no. 24, pp. 4264–4275, 2011.
- [22]. S. Amer, N. El-Wakiel, and H. El-Ghamry, *Journal of Molecular Structure*, vol. 1049, pp. 326–335, 2013.
- [23]. Danyi W., Ning L., Gui L., Kemin Y., (2006). *Science in China: Series B*. 49: 225-229.
- [24]. Kawamoto T., Nishiwaki M., Tsunekawa Y., Nozaki K., Konno T., (2008). *Inorg. Chem.* 47: 3095–3104.
- [25]. Jorgensen K. A., (1989), *Transition metal catalyzed epoxidations*. *Chem. Rev.* 89: 431-458.
- [26]. Holm R. H., (1987), *Metal-centered oxygen atom transfer reactions*. *Chem. Rev.* 87: 1401-1449.
- [27]. Temel H., Hosgoren H. Temel H., Hosgoren H., (2002). *Trans. Met. Chem.* 27: 609-612.
- [28]. Habibi M. H., Mardani M., (2015). *Spectrochim. Acta: Part A*. 137: 67-270.
- [29]. [28] H.-P. Zeng, T.-T. Wang, X.-H. Ouyang, Y.-D. Zhou, H.-L. Jing, G.-Z. Yuan, D.-F. Chen, S.-H. Du, H. Li, J.-H. Zhou. *Bioorg. Med. Chem.*, 14, 5446 (2006).
- [30]. J. Deng, T. Sanchez, L.Q. Al-Mawsawi, R. Dayam, R.A. Yunes, A. Garofalo, M.B. Bolger, N. Neamati. *Bioorg. Med. Chem.*, 15, 4985 (2007).
- [31]. E.R. Jarvo, B.M. Lawrence, E.N. Jacobsen. *Angew. Chem. Int. Ed.*, 44, 6043 (2005).
- [32]. M. Zhao, C. Zhong, C. Stern, A.G.M. Barrett, B.M. Hoffman. *J. Am. Chem. Soc.*, 127, 9769 (2005).
- [33]. T.G. Roy, S.K.S. Hazari, B.K. Dey, H.A. Miah, C. Bader, D. Rehder. *Eur. J. Inorg. Chem.*, 4115 (2004).
- [34]. A.K. Mishra, S.B. Mishra, N. Manav, D. Saluja, R. Chandra, N.K. Kaushik. *Bioorg. Med. Chem.*, 14, 6333 (2006).
- [35]. Pfaller M.A. et al, vol. 26, pp. 1437-1441, 1988.
- [36]. National Committee for Clinical Laboratory Standards. Reference method for broth dilution antifungal susceptibility testing of conidium-forming filamentous: proposed standard M38-A. Wayne, PA, USA, 2002.
- [37]. National Committee for Clinical Laboratory Standards. Method for antifungal disc diffusion susceptibility testing of yeast: proposed guideline M44-P. Wayne, PA, USA, 2003.
- [38]. Mahmoud W.H. et al, " *Spectrochim. Acta A. J. Mol. Biomol. Spectrosc.*, vol. 122, pp. 598-608, 2014.
- [39]. Sakryan I. et al, *BioMetals*, vol. 17, pp. 115-120, 2004.
- [40]. Mahmoud W.H. et al, *Appl. Organometal. Chem.*, vol. 30, pp. 221-230, 2016.
- [41]. Linert A.A. and Abou-Hussein W., *Spectrochim. Acta A*, vol. 141, pp. 223-232, 2015.
- [42]. Abo-Aly M.M. et al, *Spectrochim. Acta A*, vol. 136, pp. 993-1000, 2015.
- [43]. Shafaatian B. et al, *Spectrochim. Acta A*, vol. 5, pp. 248-255, 2014.
- [44]. El-Sonbati A.Z. et al, *Journal of Molecular Liquids*, vol. 218, pp. 434-456, 2016.
- [45]. Mahmoud W.H. et al, *Appl. Organometal. Chem.*, vol. Accepted manuscript, 2016.
- [46]. Kumar G. et al, *Journal of Molecular Structure*, vol. 1108, pp. 680-688, 2016.
- [47]. Joseyphus R.S. and Nair M.S., *J. Mycobiology*, vol. 36, pp. 93-98, 2008.
- [48]. Siji V.L. et al, " *Transition Metal Chemistry*, vol. 36, pp. 417-424, 2011.
- [49]. Tu'rkkan B. et al, " *Transition Metal Chemistry*, vol. 36, pp. 679-682, 2011.
- [50]. Mohammad Habib et al, *J. of Molecular Structure*, vol. 1143, pp. 424-430, 2017.

Walaa H. Mahmoud" Zinc complexes of novel Schiff bases derived from 1,8-Diaminonaphthalene: Synthesis, characterization and biological activity evaluation" *International Journal of Modern Engineering Research (IJMER)*, vol. 08, no. 11, 2018, pp 53-61